paper no. 55-SA-13

The American Society of Mechanical Engineers

29 WEST 39TH STREET, NEW YORK 18, NEW YORK

FLOW OF A COMPRESSIBLE FLUID IN A THIN PASSAGE

S. K. Grinnell
Assistant Supervisor, Design Division
Dynamic Analysis & Control Laboratory
Massachusetts Institute of Technology
Cambridge, Mass.

Contributed by the Machine Design Division for presentation at the ASME Diamond Jubilee Semi-Annual Meeting, Boston, Mass. - June 19-23, 1955. (Manuscript received at ASME Headquarters March 4, 1955.)

Written discussion on this paper will be accepted up to July 26, 1955.

(Copies will be available until April 1, 1956)

ABSTRACT

Pressure distribution and weight-flow rate can be predicted for laminar compressible-fluid flow in a thin passage by use of the methods presented in this paper. A simplified method can be used readily when the fluid forces due to viscous action predominate over those due to acceleration of the fluid. A more complicated trial-and-error method seems to be required for larger passages where, though the flow may be laminar, the momentum effects due to acceleration of the compressible fluid are appreciable. An experimental apparatus was used to examine the validity of the analytical work. Experimental pressure distributions agree within a maximum deviation of 10 per cent with the theoretical distributions predicted by both the comprehensive and simplified theories. Experimental weight-flow rates agree within a maximum deviation of 50 per cent with predictions of the simplified theory. Dimensionless plots of pressure distribution are presented with experimental curves of flow rate versus pressure ratio for various ratios of passage length L to passage height h. These plots, together with simple equations, have been prepared for direct use by the designer.

1256--55

FLOW OF A COMPRESSIBLE FLUID IN A THIN PASSAGE

by S. K. Grinnell

NOMENCLATURE

The following nomenclature is used in the paper:

A = cross-sectional area of passage, sq. in.

A_ω = wall area, sq. in.

b = width of passage transverse to flow, in.

c = speed of sound, ips

c_p = specific heat of gas at constant pressure, sq in./sec^2-deg R

D = hydraulic diameter, in.

f = friction factor

g = acceleration due to gravity, in/sec^2

h = height of passage, in.

k = ratio of specific heats

L = length of passage in direction of flow, in.

M = Mach number

P = pressure, psi

Q = volume rate of flow, in.^{3}/sec

R = universal gas constant, sq in./sec^2-deg R

Re = Reynolds numbers

T = temperature, deg R

u = fluid velocity, ips

V = fluid velocity, ips

x = distance along passage in flow direction, in.

y = distance from center line of passage transverse to flow, in.

μ = viscosity lb-sec/sq in.

ρ = density, lb-sec^2/in.^{4}

τ = fluid shear stress, psi

τ_ω = fluid shear stress at wall, psi

ω = weight flow rate, lb/sec

INTRODUCTION

With current interest and activity in the development of pneumatic components and systems, there is a need for basic information in readily usable form concerning the flow of compressible fluids in various types of flow passages. Designers of pneumatic mechanisms require information that will enable them to predict leakage flows and the distribution of pressure along leakage-flow paths. Flow past rotating and stationary shafts, flow in "hydrostatic" air bearings, leakage flow in control valves, and the flow in pneumatic resistance elements are examples of where this need has become apparent.

The general problem of gas-leakage flows in narrow channels of constant cross-sectional area was treated by A. Egli (1)[1] in 1937, with special attention to the case of leakage flows past the stems of air and steam valves. G. L. Shires (2) has also treated the flow in a narrow slot with particular reference to the problem of a "hydrostatic" compressible-fluid bearing. The work to be described in this paper is part of a thesis investigation (3) on the design of "hydrostatic" air bearings.

The problem treated here is that of compressible fluid flow in a thin passage, as shown in Fig. 1. The width b of the flow passage transverse to the direction of flow is of the same order of magnitude as the length of the passage in the direction of flow L, and the ratio of the height of the passage h to the length L is very small. For this range of geometric parameters, flow may be considered laminar and essentially one-dimensional. As the analyses and experimental work demonstrate, the viscous-shearing forces predominate over acceleration forces when the ratio of height to length h/L is very samll, but the momentum forces associated with the acceleration of the fluid become more important as h/L becomes larger.

ANALYSES

Adiabatic, Constant-Area Flow of a Compressible Fluid with Friction

A comprehensive analysis which has been given by A. Shapiro (4) for the flow of a compressible fluid in a constant-area passage includes the effects of temperature change as well as friction and momentum effects acting in the fluid. However, the solution is not in the form of explicit relationships that may be used directly for design purposes. Solutions to many problems associated with this type of flow must be found by a trial-and-error process because the stream properties and flow rate are interdependent in a nonlinear way.

The purpose of this analysis is to show how the stream properties vary along the length L of a duct of constant width b and constant height h.

The principal assumptions are:

1 The flow is one-dimensional and steady.

2 The working fluid is a perfect gas.

3 There are no external heat or work effects, and differences in elevation are negligible.

---

[1] Underlined numbers in parentheses refer to the Bibliography at the end of the paper.

Two sections of the duct are considered to be an infinitesimal distance dx apart as shown in Fig. 2(a).

If a perfect gas relation is assumed,

$$P = \rho RT \quad \ldots\ldots\ldots\ldots\ldots \quad (1)$$

then by logarithmic differentails

$$\frac{dP}{P} = \frac{d\rho}{\rho} + \frac{dT}{T} \quad \ldots\ldots\ldots\ldots \quad (2)$$

From the definition of the Mach number

$$M = \frac{V}{c} \text{ or } M^2 = \frac{V^2}{kRT} \quad \ldots\ldots\ldots\ldots\ldots \quad (3)$$

where

$$c = \text{sound velocity} = \sqrt{\frac{kP}{\rho}} = \sqrt{kRT} \quad \ldots \quad (4)$$

the following equation is obtained

$$\frac{dM^2}{M^2} = \frac{dV^2}{V^2} - \frac{dT}{T} \quad \ldots\ldots\ldots\ldots\ldots \quad (5)$$

The energy equation of steady, adiabatic flow of a perfect gas is written

$$c_p dT + \frac{dV}{2} = 0 \quad \ldots\ldots\ldots\ldots\ldots \quad (6)$$

By dividing through by $c_p T$, and by using the definition of Mach number, where $c_p = kR/(k-1)$, Equation (6) becomes

$$\frac{dT}{T} + \frac{k-1}{2} M^2 \frac{dV^2}{V^2} = 0 \quad \ldots\ldots\ldots\ldots\ldots \quad (7)$$

The continuity equation is

$$\frac{\omega}{A} = \rho g V = \text{const} \quad \ldots\ldots\ldots\ldots\ldots \quad (8)$$

Since A is constant, with use of logarithmic differentials

$$\frac{d\rho}{\rho} + \frac{dV}{V} = 0 \quad \ldots\ldots\ldots\ldots\ldots \quad (9)$$

or since

$$\frac{dV}{V} = \frac{1}{2}\left(\frac{dV^2}{V^2}\right) \quad \text{..... (10)}$$

$$\frac{d\rho}{\rho} = \frac{1}{2}\left(\frac{dV^2}{V^2}\right) = 0 \quad \text{..... (11)}$$

From Fig. 2(a), the momentum equation is written

$$-AdP - \tau_\omega dA_\omega = \frac{\omega}{g} dV \quad \text{..... (12)}$$

where A is the cross-sectional area, τ_ω is the shear stress exerted on the stream by the walls, and dA_ω is the wall area over which τ_ω acts.

Now the drag coefficient, or friction factor f, is the ratio of the shear stress to the dynamic head of the stream and is a measure of the relative significance of viscous and momentum effects

$$f = \frac{\tau_\omega}{\frac{\rho V^2}{2}} \quad \text{..... (13)}$$

The hydraulic diameter D is defined as four times the ratio of cross-sectional area to wetted perimeter

$$D = 4\,\frac{A}{dA_\omega}\,dx \text{ or } dA_\omega = \frac{4Adx}{D} \quad \text{..... (14)}$$

When Equations (8), (13), and (14) are introduced into Equation (12)

$$-dP - 4f\rho\frac{V^2}{2}\frac{dx}{D} = \frac{\omega}{gA}dV = \rho V^2\frac{dV}{V} \quad \text{..... (15)}$$

By dividing by P, where $V^2 = kPM^2$, and by using Equation (10)

$$\frac{dP}{P} + \frac{kM^2}{2}\,4f\frac{dx}{D} + \frac{kM^2}{2}\frac{dV^2}{V^2} = 0 \quad \text{..... (16)}$$

The five simultaneous equations, namely, Equations (2), (5), (7), (11), and (16), may be combined to give the differential equations for P and M as functions of 4F dx/D

$$\frac{dM^2}{M^2} = kM^2\left(\frac{1 + \frac{k-1}{2}M^2}{1 - M^2}\right)4f\frac{dx}{D} \quad \text{..... (17)}$$

$$\frac{dP}{P} = - kM^2 \left[\frac{(1 + (k-1) M^2)}{2 (1 - M^2)} \right] 4f \frac{dx}{D} \quad \ldots\ldots\ldots\ldots\ldots\ldots \quad (18)$$

By first integrating differential Equation (17), M can be found as a function of x, if f is assumed to be constant

$$\int_0^L 4f \frac{dx}{D} = \int_{M_1}^{M_2} \frac{1 - M^2}{k M^2 (1 + \frac{k-1}{2} M^2)} dM^2 \quad \ldots\ldots \quad (19)$$

The limits are as follows:

1 The entrance where Mach number is M_1 and x is zero.

2 The section a distance L along the passage where Mach number is M_2.

The integration for the special case where the final Mach number is unity gives

$$\left(\frac{4fL_{max}}{D} \right) = \frac{1-M^2}{kM^2} + \frac{k+1}{2k} \ln \left[\frac{(k + 1) M^2}{2 (1 + \frac{k-1}{2} M^2)} \right] \quad \ldots\ldots\ldots\ldots \quad (20)$$

where L_{max} is the length required to attain a final Mach number of unity. Since 4fL/D is a function of Mach number only, the length of duct for a flow to pass from Mach number M_1 to M_2 can be found from

$$\frac{4fL}{D} = \left(\frac{4fL_{max}}{D} \right)_{M_1} - \left(\frac{4fL_{max}}{D} \right)_{M_2} \quad \ldots\ldots\ldots\ldots\ldots \quad (21)$$

where f is a mean friction factor.

If the passage length L is greater than L_{max}, flow will be "choked," with the result that M_1 and flow rate decrease as L is increased. The exit Mach number M_2 will be unity for L equal to or greater than L_{max}.

The expression for dP/P can be integrated similarly once M is known as a function of x, in order to find the pressure distribution along the passage. These expressions relating the Mach number, pressure, length of passage, and friction factor have been tabulated in Table 42 of the Gas Tables (5).

If friction factor f as a function of Reynolds number Re, inlet pressure P_1, outlet pressure P_2, and the dimensions of the passage L, h, and b are known, the flow rate and pressure distribution can be found by referring to Table 42. An exit Mach number of unity is first assumed. The pressure ratio P_1/P_2 is then equal to P/P^* in Table 42, where P^* is the pressure when Mach number is unity, and for this value of P_1/P_2 there is an entering Mach number M_1 and $(4fL_{max}/D)_{M_1}$. From M_1 and a knowledge

of T_1, V_1 can be calculated from Equation (4). For this value of V_1 and a corresponding Reynolds number, there is a value of friction factor f. With the dimensions L and h, where $2h = D$, $4fL/D$ can be obtained. If this number is equal to $(4fL_{max}/D)_{M_1}$, the exit Mach number M_2 is unity. If $4fL/D$ is less than $(4fL_{max}/D)$, the exit Mach number M_2 is less than unity. If $4fL/D$ is subtracted from $(4fL_{max}/D)_{M_1}$ to obtain $(4fL_{max}/D)_{M_2}$, the corresponding M_2 and $(P/P^*)_2$ can be found. If $4fL/D$ is greater than $(4fL_{max}/D)_{M_1}$, the flow is choked, and by trial-and-error, a new $4fL/D$ must be found such that $(4fL_{max}/D)_{M_1}$ and $4fL/D$ are equal for new values M_1 and $(P/P^*)_1$.

For any of the three cases, the flow rate is then

$$\omega = \rho_1 g b h V_1$$

and pressure distribution can be found by using intermediate values of P/P^* and $4fL_{max}/D$.

Simplified Analysis Neglecting Momentum Effects

A simplified analysis that neglects momentum effects leads to explicit relationships for pressure distribution and flow rate. The Hagen-Poiseuille analysis which assumes that wall-friction forces are predominant is developed for a compressible fluid in a thin passage. The assumptions are as follows

1 Viscous-shear forces govern the flow to the extent that momentum forces can be neglected.

2 The flow is laminar and fully developed.

3 Temperature is constant throughout the flow.

From Fig. 3, showing an element of fluid acted on by shear-stress and pressure forces, the static equilibrium equation can be written as

$$2Pby - (P-dP)2by - 2\tau\, bdx = 0 \quad \ldots\ldots\ldots\ldots \quad (22)$$

By Newton's (6) law of viscous flow

$$\tau = -\mu \frac{du}{dy} \quad \ldots\ldots\ldots\ldots\ldots\ldots\ldots \quad (23)$$

where u is the velocity of a particle at a distance y from the center of the passage, μ is viscosity, and τ is the shear stress. When Equations (22) and (23) are combined

$$du = -\frac{y}{\mu}\, dy\, \frac{dp}{dx} \quad \ldots\ldots\ldots\ldots\ldots\ldots \quad (24)$$

By integrating u with respect to y and by substituting the limits $y = h/2$, $u = 0$, the equation of the velocity distribution is

$$u = \left(\frac{h^2}{8} - \frac{y^2}{2}\right)\frac{1}{\mu}\, \frac{dp}{dx} \quad \ldots\ldots\ldots\ldots\ldots\ldots \quad (25)$$

This is a parabolic distribution, as shown in Fig. 3.

The area for flow is 2by for an increment of flow dQ so that

$$dQ = \frac{2by}{\mu}\left(\frac{h^2}{8} - \frac{y^2}{2}\right)\frac{dp}{dx} \quad \ldots\ldots\ldots\ldots\ldots\ldots \quad (26)$$

Integrating the flow over the entire flow area, putting in limits, simplifying, and adding a minus sign because dp/dx is negative in the direction of flow yield

$$Q = -\frac{bh^3}{12\mu}\frac{dp}{dx} \quad \ldots\ldots\ldots\ldots\ldots\ldots\ldots\ldots \quad (27)$$

The equation for weight-flow rate now can be written

$$\rho g Q = \quad = -\frac{gbh^3}{12\mu}\frac{dp}{dx} \quad \ldots\ldots\ldots\ldots\ldots\ldots \quad (28)$$

Introduction of the perfect gas law

$$\frac{P}{\rho} = RT \quad \ldots\ldots\ldots\ldots\ldots\ldots \quad (29)$$

yields

$$\omega = -\frac{gbh^3 P}{12\mu RT}\frac{dp}{dx} \quad \ldots\ldots\ldots\ldots\ldots\ldots \quad (30)$$

Whe weight-flow rate is constant over any cross section and because of the assumption of constant temperature, the viscosity, which is principally temperature-dependent, will remain constant. Then integration to find the pressure P at any point along the flow path gives

$$P = \sqrt{P_1^2 - \frac{24\mu RTwx}{gbh^3}} \quad \ldots\ldots\ldots\ldots\ldots\ldots \quad (31)$$

Therefore, the pressure distribution in the direction of flow is parabolic.

By use of the same relationships to find weight-flow rate, integration over the length of the flow path L gives

$$\omega = \frac{gbh^3}{24 RTL}\left(P_1^2 - P_2^2\right) \quad \ldots\ldots\ldots\ldots\ldots\ldots \quad (32)$$

From Equation (32) the weight-flow rate can be computed if the end conditions and geometry of the flow path are known.

EXPERIMENTAL APPARATUS

In order to investigate experimentally the pressure distribution and flow through a thin passage between flat plates, a simple fixture with a movable plate and a fixed plate each 6 1/4 in. wide and 4 in. long was designed, as shwon in Fig. 4.

The material used in the flow-boundary surfaces was SAE 1045 hot-rolled steel stabilized by normalizing before rough and finish machining. The surfaces of the two plates were lapped together to produce very fine flat surfaces which were given a black-oxide finish to protect them from corrosion. The resulting bright black finish had a surface roughness less than 4 μin. rms.

As shown in Fig. 4, all parts of the apparatus were made heavy enough to minimize the possibility of deflections that would invalidate the results of the experimental work.

The movable plate, which is 3/4 in. thick, has an O-ring around its circumference to seal against leakage between it and the annular ring into which it fits with approximately 0.005-in. clearance all around. A second O-ring seals the space between the annular ring and the 1 1/2-in.-thick base plate.

Three differential screws provide the adjustment for the separation between the flow plates, and 3-dial indicators measure the plate separation. The differential screws have a No. 6-40 thread which mates with a hole in the movable plate and a No. 8-36 thread which mates with a tapped hole in a stationary arm attached to the base plate. This arrangement, providing a motion of 1/400 in. per revolution of the screw, allows fine adjustment of the passage height h.

A grid of 81-1/32-in-diam pressure-tap holes consisting of 9 rows of 9 holes each on 1/2-in. centers in the direction of flow and 5/8-in. centers at right angles to the direction of flow cover the stationary base plate. A manifolding plate, which was lapped with the underside of the base plate after grinding to give a sealing surface, can be located by means of a rack-and-pinion arrangement to lead out pressures from 18 points, 9 from each end of the manifold plate. The apparatus schematic of Fig. 5 shows the vernier arrangement providing 5 positions in which 2 rows of holes are synchronized to feed pressures to the ends of the manifold plate. This system of pressure-tap manifolding permitted the use of 18 mercury manometers for pressure measurements instead of the 82 which would have been required without the manifold.

Two sets of three 1/2-in-diam tubes lead into opposite pressure chambers through the sides of the base plate to feed air in and out of the apparatus. The pressure chambers are 5/16 by 1/2 by 6-1/4 in., providing large enough volume so that flow velocities before and after the flow plate restriction are negligible.

INSTRUMENTATION

A schematic diagram of the general instrumentation and air supply and exhaust arrangement is shown in Fig. 5.

Three dial indicators with 4-in. dials and 0.001-in. graduations were used to measure the separation between the plates.

Eighteen vacuum-type manometers were used to measure the pressure distribution. The vacuum-manometer board, shown in the photograph of Fig. 4 and drawn schematically in Fig. 5, has a large reservoir of mercury maintained at atmospheric pressure. The operating supply pressures for the tests ranged from 2/3 atm to 2 atm on the upstream side and from 1 atm down to 1/10 atm on the downstream side. The mercury manometers could be read to within 1/20 in. of mercury or approximately 1/40 psi.

A calibrated orifice flowmeter constructed according to ASME Standards was used to measure weight-flow rate. The pressure taps before and after the orifice were connected to a differential water manometer and also to separate absolute-pressure mercury manometers.

Iron-constantan thermocouples were placed in both the upstream and downstream chambers to measure the temperature at entrance and exit of the flow passage. A Leeds-Northrop Wheatstone bridge potentiometer circuit was used to measure the thermocouple potential within 0.1 mv.

A pressure tap was placed in both the upstream and downstream pressure chambers to determine the end pressures. These taps were connected to mercury U-tube manometers that could measure as high as 2 atm or as low as perfect vacuum.

The upstream side of the apparatus was connected through orifice flowmeter, valve, and flexible hose to a 125-psi air compressor. The downstream side of the apparatus was connected through a valve to a steam ejector which is capable of handling 0.2 lb of air per second at a pressure of 2 psia. The capacities of both compressor and ejector were more than adequate for this work because flows of less than 0.01 lb/sec were used at all times.

OPERATION AND DATA

Pressure distribution and weight-flow rate data were taken with the flat-plate apparatus for operating pressure ratios P_1/P_2 in the range from 2 to 12. Clearance ratio h/L was varied between 1/4000 and 1/667.

The streamlines were determined to be very nearly parallel in the major flow direction by means of very fine oil lines on the test plates made in one set of runs.

A set of runs was made with shims determining the plate separation as a check on the accuracy of the settings read from the dial indicators used for determining plate separation in the major portion of the runs.

RESULTS

The pressure distributions calculated from both the comprehensive and simplified analyses are compared with experimentally measured distributions in Fig. 6 and 7. The simple theory is seen to be good for very small h/L ratios in the range from 1/1000 to 1/4000, as given in Fig. 6. For the extremely small clearances involved, the momentum effects can be neglected, and the simplified theory used to predict the pressure distribution. For very small clearances, the quantity $4fL_{max}/D$ becomes very large, and errors in using Table 42 of the Gas Tables (5) are large, with the result that the comprehensive method does not give very accurate results.

However, as the clearance is increased to where h/L is 1/667, as shown in Fig. 7, the pressure distribution predicted by the simplified equation does not agree as well with the experimental pressure distribution. For these larger ratios, the complete analysis prediction of pressure distribution based on Shapiro's methods (4) agrees well with the experimental pressure distribution.

The weight-flow rate, which is predicted to be a function of the passage height cubed h^3 by the simplified theory, Equation (32), is found experimentally to be somewhat different, as shown in Fig. 8. It would be expected that for large h/L ratios where momentum effects are important the experimental weight-flow rates would be smaller than those predicted by the simplified theory.

Experimental weight-flow rates obtained for various h/L ratios as a function of pressure ratio (P_1/P_2) are presented in Fig. 9 for a passage 1-in. long and 1-in. wide.

A plot of experimentally obtained friction factor f versus Reynolds number is given in Fig. 10. The friction factors calculated from the experimental weight-flow rates agree reasonably well with the work of Egli (1), as is illustrated by a comparison of the curves of Fig. 10.

CONCLUSIONS

A parabolic pressure distribution is accurate for passage height-to-length ratios of 1/1000 and smaller where momentum effects can be neglected and viscous forces predominate. For this same range of passage height-to-length ratios, the simplified relationship that weight-flow rate as a function of passage height cubed proves reasonably accurate.

For larger passage height-to-length ratios where the flow is laminar, the pressure distribution and weight-flow rate can be predicted by using the methods which account for momentum effects. The table of friction factor versus Reynolds number (Fig. 10) and Table 42 of the Gas Tables (5) facilitate calculations.

ACKNOWLEDGMENT

The author is indebted to Prof. J. A. Hrones and the Dynamic Analysis and Control Laboratory for making this paper possible.

Prof. J. L. Shearer encouraged and counseled the author with valuable assistance throughout all stages of the investigation.

The work reported here was supported by the Bureau of Ordnance, United States Navy, Contract NOrd 9661 with the Division of Industrial Cooperation, Massachusetts Institute of Technology.

BIBLIOGRAPHY

1 "The Leakage of Gases Through Narrow Channels," by A. Egli, Trans. ASME, vol. 59, 1937, p. A-63.

2 "The Viscid Flow of Air in a Narrow Slot," by G. L. Shires, National Gas Turbine Establishment Memo No. 46, December 1948, Farnborough, England.

3 "A Study of Pressurized Air Bearing Design, Steady Loading - No Rotation," by S. K. Grinnell, M. I. T., Department of Mechanical Engineering, S. M. thesis, January 1954, Cambridge, Mass.

4 "Flow of Compressible Fluids," by A. H. Shapiro, Notes for M. I. T., Department of Mechanical Engineering, Course 2.491, Cambridge, Mass. 1952.

5 "Gas Tables," by J. H. Keenan and J. Kay, John Wiley and Sons, Inc., New York, N Y., 1945.

6 "The Mathematical Principles of Natural Philosophy," by I. Newton, J. Maclehose, Glasgow, 1871.

CAPTIONS FOR ILLUSTRATIONS

Fig. 1 Fluid flow in a thin passage

Fig. 2 Element of fluid

Fig. 3 Element of fluid

Fig. 4 Experimental fixture

Fig. 5 Experimental apparatus

Fig. 6 Dimensionless plot of pressure distribution

Fig. 7 Dimensionless plot of pressure distribution

Fig. 8 Weight flow rate versus passage height

Fig. 9 Weight flow rate versus pressure ratio

Fig. 10 Friction factor versus Reynolds number

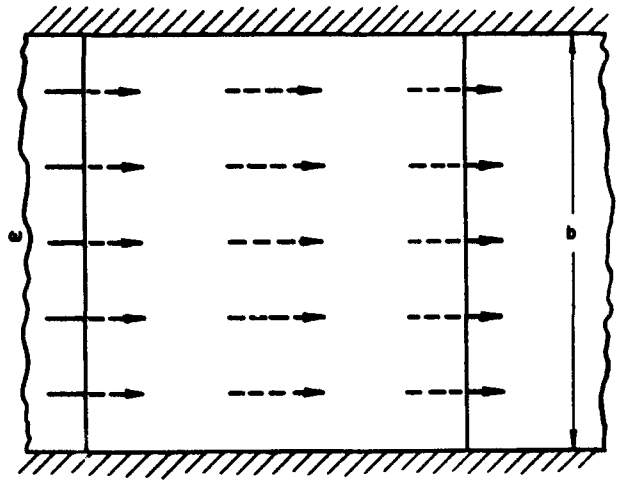

Fig.4

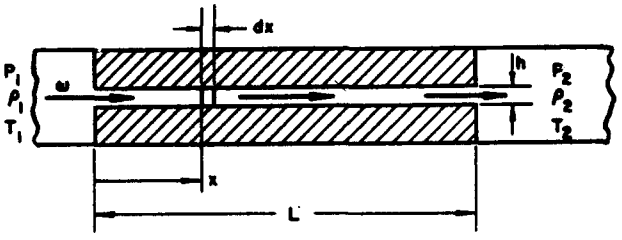

Fig.1

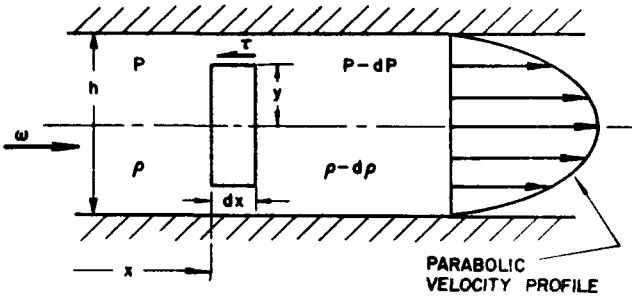

Fig.3

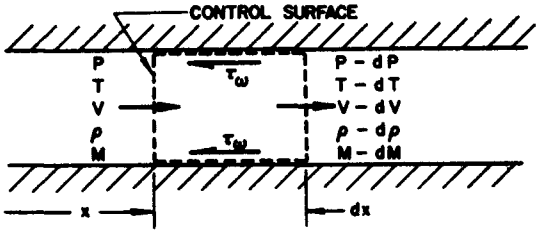

Fig.2

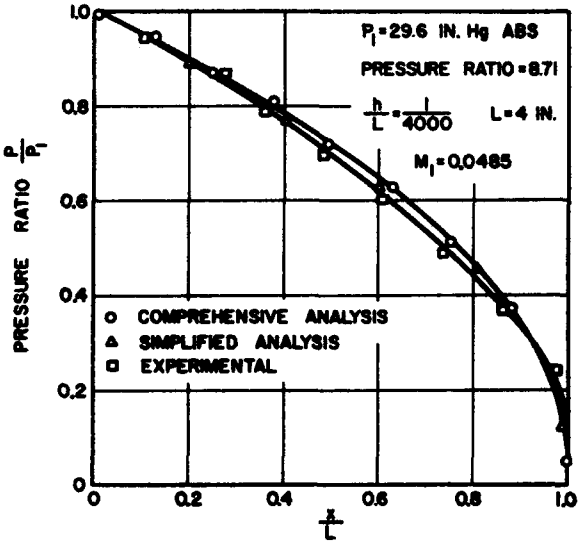

Fig.6

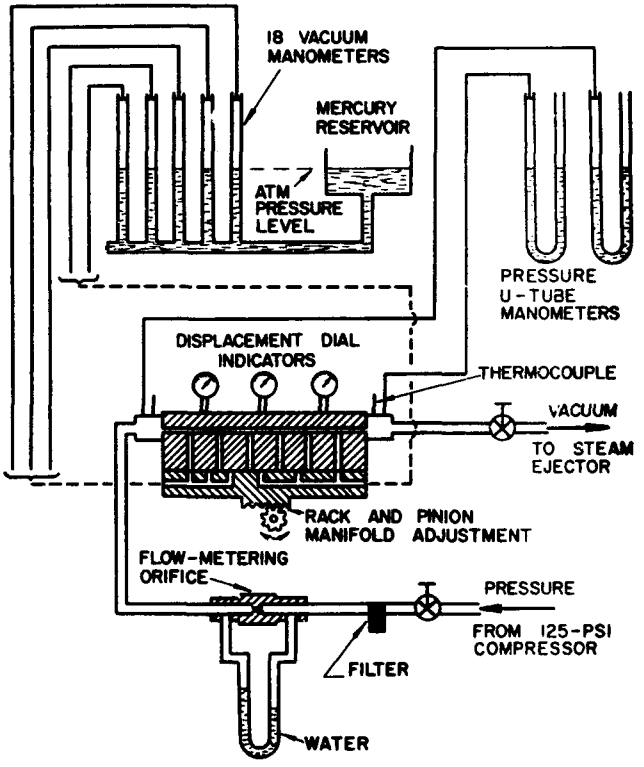

Fig.5

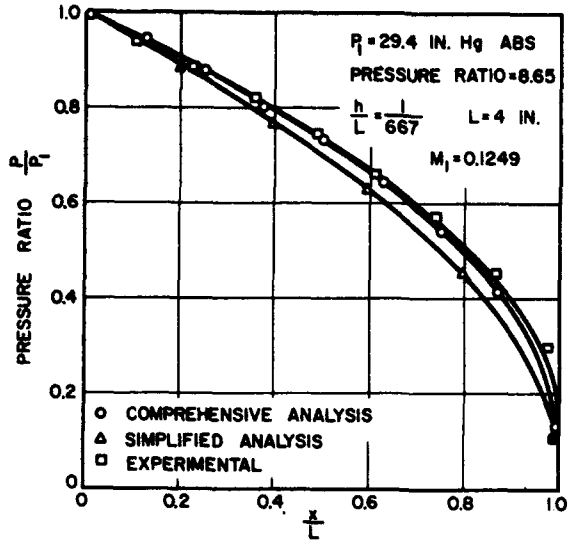

Fig.7

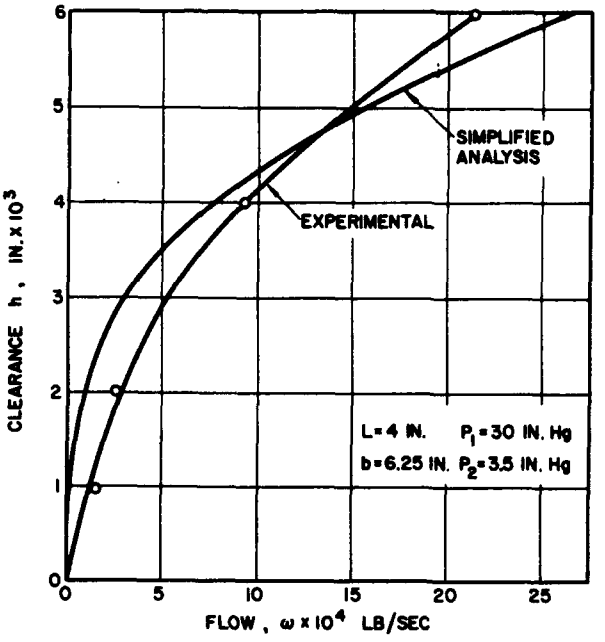

Fig.8

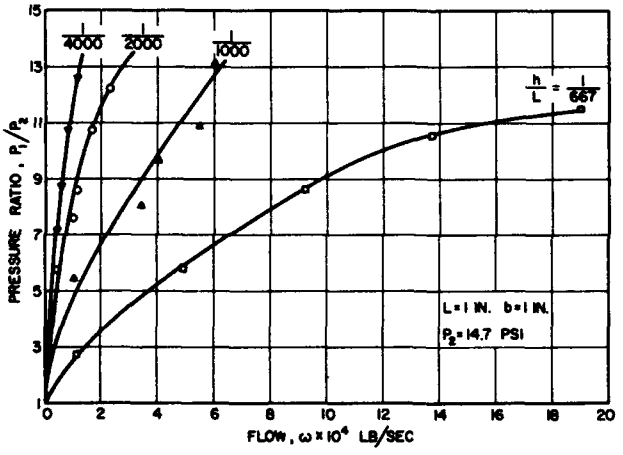

Fig.9

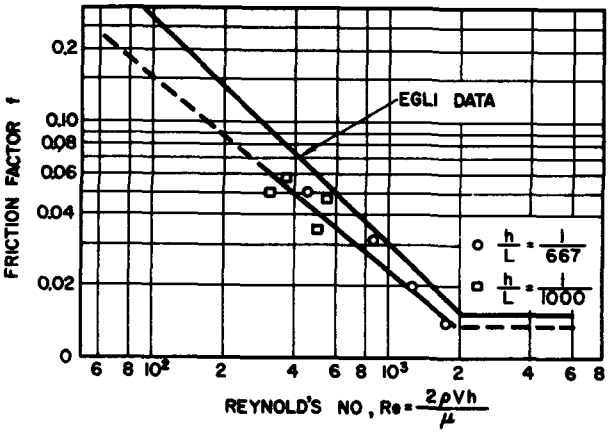

Fig.10